An Adaptive Fast Charging Strategy Considering the Variation of DC Internal Resistance

Yipei Wang, *Graduate Student Member, IEEE*, Ancheng Liu, Yaochen Zhu, Hailong Zhang, *Member, IEEE*, Yafei Chen, *Member, IEEE*, and Sung-Jun Park, *Member, IEEE*

***Abstract*—In this article, an adaptive fast charging strategy for lithium-ion batteries considering the variation of dc internal resistance (DCIR) is proposed, which applies to mobile applications. The experiments prove that the DCIR obeys the Gaussian distribution during the normal charging stage. However, the DCIR no longer obeys Gaussian distribution once the battery is fully charged. The proposed strategy employs the maximum-likelihood method to estimate the expectation and variance of the Gaussian distribution. The charging mode switches from constant current (CC) to constant voltage (CV) immediately when the DCIR deviates significantly from the expectation. Under the premise of satisfying the high accuracy for the parameter estimates, a constrained optimization problem is established to determine the DCIR minimum number of measurements ($n_{\min}$), and the constraints are transformed into hypothesis testing for solving. The CC operating time is maximized based on $n_{\min}$ and the adaptive control of the transition point. The experiments verify the validity of the proposed method. The results show that compared with the CC-CV method, the proposed strategy saves 52.2%, 41.57%, and 29.72% of the charging time at 1C, 0.75C, and 0.5C, respectively, which effectively improves the charging speed and prevents overcharging.**

***Index Terms*—Adaptive control, constrained optimization, dc internal resistance (DCIR), fast charging, maximum-likelihood estimation.**

I. Introduction

LITHIUM-ION (Li-ion) batteries have been regarded as an energy storage solution for applications, such as mobile electronic equipment and electric transportation, due to their high power density, long cycle life, and low self-discharge [1]. However, one of the main obstacles limiting these applications is the anxiety of consumers regarding the prolonged charging process of Li-ion batteries. Customers hope that the Li-ion batteries operate longer after charge, but since battery volume cannot increase indefinitely, it is a natural solution to provide a faster charge speed [2]. Charging time directly impacts the consumer's subjective perception and is crucial to the promotion of commodities, such as mobile electronic equipment and electric vehicles. As the demand for Li-ion batteries grows, fast charging strategies are attracting more and more attention in the pursuit of speed while also maximizing battery safety for optimal performance and extended life [3], [4].

The constant current and constant voltage (CC-CV) mode is the mainstream charging method nowadays. It adopts CC charging at first until the terminal voltage reaches the cutoff voltage, and then keeps that voltage constant for charging. In the CC stage, if the C-rate of the charging current is 1C, it is defined as the current for charging the battery to the rated capacity in one hour. In the CV stage, the current gradually decreases as the battery capacity increases, the charging ends once the current reduces to a certain threshold, which ensures the battery is fully charged and prevents overcharging effectively. However, the CC-CV method results in a long charging time. The CV stage is actually the major factor limiting the charging speed due to the lower current [5], [6]. The charging of Li-ion batteries is a complex process with multiple factors coupled. The factors include environmental temperature, state of charge (SOC), state of health (SOH), C-rate, and internal materials. The empirical approach of simply increasing the C-rate or overcharging beyond the cutoff voltage would cause irreversible damage to the cycle life, so it is not an ideal solution.

In recent years, many related studies have been carried out on the fast charging strategy of Li-ion batteries. A built-in resistance (BIR) detection circuit was designed in [7], and the CC operation time was extended by detecting the BIR, but there were no specific parameters or calculation procedures for the transition point. Anseán et al. [8], [9] proposed a multistage fast charging method that divides the charging process into three stages, containing two CC stages and one CV stage. It is also pointed out that the proposed method enables fast and safe charging effectively and without affecting the long-term cycle performance. A multistage CC charging method (MSCC) with fast charging capability was proposed in [10], where the MSCC employs only CC with different amplitudes without the CV stage. For MSCC,

Manuscript received 23 June 2022; revised 4 October 2022 and 16 November 2022; accepted 17 December 2022. Date of publication 21 December 2022; date of current version 14 February 2023. This work was supported in part by the Gwangju Jeonnam Local Energy Cluster Manpower training of the Korea Institute of Energy Technology Evaluation and Planning under Grant Korea Government Ministry of Knowledge Economy (20214000000560), in part by the Korean government Ministry of Trade, Industry, and Energy, and in part by the Korea Industrial Technology Promotion Agency (P0015333). Recommended for publication by Associate Editor S. Williamson. *(Corresponding author: Sung-Jun Park.)*

Yipei Wang, Ancheng Liu, Yaochen Zhu, and Sung-Jun Park are with the Department of Electrical Engineering, Chonnam National University, Gwangju 61186, South Korea (e-mail: wangy.p@qq.com; 1054924519@qq.com; 949169889@qq.com; sjpark1@jnu.ac.kr).

Hailong Zhang is with the Department of Information and Control Engineering, Qingdao University of Technology, Qingdao 266525, China (e-mail: hailong9925@gmail.com).

Yafei Chen is with the Department of Electrical and Information Engineering, Zhengzhou University of Light Industry, Zhengzhou 450002, China (e-mail: swjtuqust@163.com).

Color versions of one or more figures in this article are available at https://doi.org/10.1109/TPEL.2022.3230928.

Digital Object Identifier 10.1109/TPEL.2022.3230928

various optimization methods have been proposed, such as the Taguchi method [11], [12], fuzzy logic [13], and particle swarm optimization [14], [15]; however, these methods are based on a large number of pretests, and the charging target capacity of most studies is not 100%. Therefore, the validity in practical applications remains to be further investigated. In addition, the pulse charging method, which refers to charging the battery with high current pulses separated by a small current, is also considered a fast and effective method [16]. The proper selection of pulse amplitude, duty cycle, and frequency is essential for charging, and to minimize the charging time, it is necessary to determine the parameters of pulse charging and the impact of different parameters on the charging time according to some optimization methods [17], [18]. The pulse charging methods are relatively demanding on the computational performance of the controller and complicated to implement due to the large number of parameters involved. Several approaches considering SOH have been proposed [2], [19], [20], [21], which are based on electrochemical system modeling and predictive control algorithms with explicit constraints on the state variables in a physical sense, however, the limitation is the lack of hardware experiments to verify the validity of the strategies.

The safety and rapidity of the battery charging process are contradictory, which demands a fast charging strategy balances them. It is shown that the dc internal resistance (DCIR) of a battery varies continuously with time during charging and discharging, which is a key parameter for measuring the performance of Li-ion batteries. DCIR is significant for estimating common factors, such as available capacity, SOH, and SOC of the batteries [22], [23]. The reduction in capacity during degeneration is typically accompanied by an increase in DCIR, and batteries with low DCIR have high capacity and strong discharge capability [24], [25]. With the acquisition of accurate real-time DCIR evolution data, it is feasible to deduce the battery capacity variation, which is potentially applied to estimate the status information during charging [26]. It is possible to maximize the charging speed within a reasonable range while preventing the battery from overcharging by identifying a safe upper limit for charging based on the variation of DCIR.

Based on the above ideas, an adaptive fast charging strategy for Li-ion batteries considering the variation of DCIR is proposed in this article, which applies to mobile electronic equipment. Specifically, several critical contributions are made as follows.

1) The trend of DCIR variation during the charging process is obtained by online measurement of Li-ion batteries. The results show that the DCIR obeys the Gaussian distribution in the normal charging stage. While the DCIR shows a trend of first decreasing and then increasing sharply after the battery is fully charged.
2) The proposed strategy employs the maximum-likelihood method to estimate the expectation and variance of the Gaussian distribution obeyed by the DCIR, and the estimates are used for adaptive control of the optimal transition point. When the DCIR deviates significantly from the expectation, the battery is considered close to full charge and immediately switches from CC to CV mode.

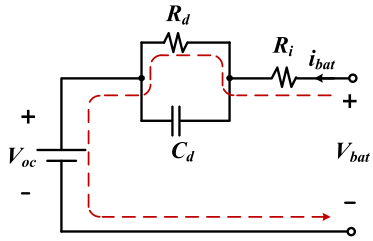

Fig. 1. Thevenin equivalent circuit model of the battery.

3) A constrained optimization problem is established to determine the DCIR minimum number of measurements ($n_{\min}$) while satisfying the premise of high accuracy for the parameter estimates. To simplify the problem, the constraints are transformed into hypothesis testing to evaluate the Gaussian distribution of the data samples.
4) The CC operating time is maximized based on $n_{\min}$ and the adaptive control of the transition point. The specific implementation of the fast charging strategy is presented. The experiments verify the validity of the proposed strategy.

The rest of this article is organized as follows. Section II is about the principle of online measurement and the trend of DCIR obtained from the measurements. Section III concerns the method for determining the optimal transition point and $n_{\min}$ and the implementation of the proposed fast charging strategy. The proposed strategy is verified and discussed by experiments in Section IV. Finally, Section V concludes this article.

II. DCIR Online Measurement of Li-Ion Batteries

A. DCIR Online Measurement

The Thevenin equivalent circuit model of the battery is shown in Fig. 1. Here, $R_{\rm i}$ is ohmic resistance, which simulates the voltage change generated instantaneously by the applied current. $R_{\rm d}$ and $C_{\rm d}$ are the polarization resistance and capacitance, respectively, which simulate the response resulting from the change of voltage with time. $i_{\rm bat}$ is the charging current, and $V_{\rm bat}$ and $V_{\rm oc}$ are the corresponding battery terminal voltage and open-circuit voltage, respectively.

The current profile and the corresponding terminal voltage of the online DCIR measurement method based on two-level CC pulses are shown in Fig. 2. The battery is first charged with CC I_1, and $V_{\rm bat}$ is equal to V_1 at the end of this stage. Then, the current steps down to I_2 for charging with a duration of t_2. A sudden shift in charging current will cause a rapid drop in $V_{\rm bat}$ first due to $R_{\rm i}$. After that, $V_{\rm bat}$ will keep falling slowly. It is because the voltage on $C_{\rm d}$ cannot change abruptly after the current drops, and $C_{\rm d}$ will discharge slowly through $R_{\rm d}$. The stable value of $V_{\rm bat}$ at the end of this stage is V_2. During CC mode, the current flows through $R_{\rm i}$ and $R_{\rm d}$ to charge the battery, as shown by the red dashed line in Fig. 1. Since the duration of the test process is relatively brief, it is assumed that $V_{\rm oc}$ and DCIR have not changed, so V_1 and V_2 can be represented respectively as

$$\begin{cases} V_1 = V_{\rm oc} + I_1 \left(R_{\rm d} + R_{\rm i}\right) \\ V_2 = V_{\rm oc} + I_2 \left(R_{\rm d} + R_{\rm i}\right) \end{cases}. \tag{1}$$

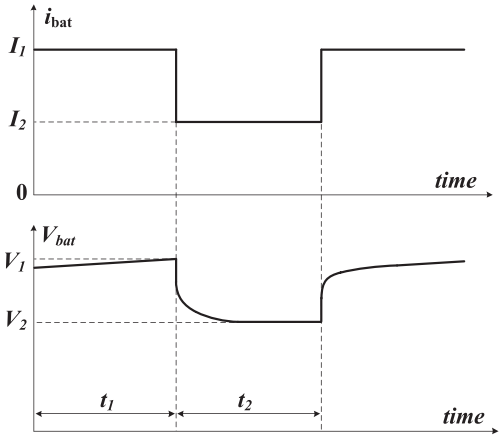

Fig. 2. Current profile and corresponding terminal voltage of the online DCIR measurement based on two-level CC pulses.

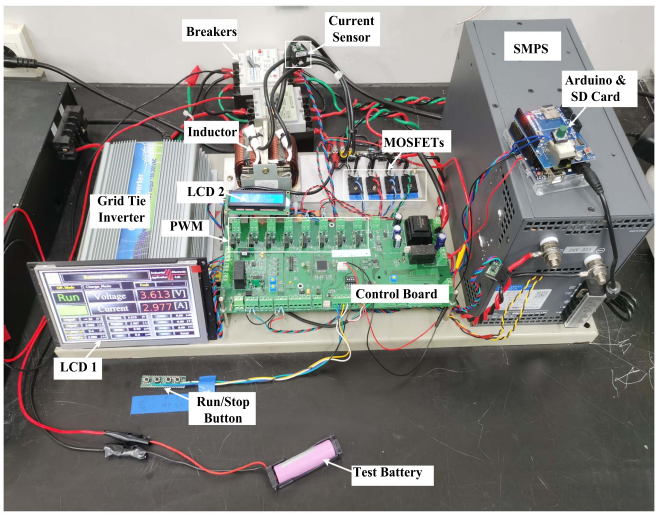

Fig. 3. Experimental setup for DCIR online measurement.

DCIR is calculated by the following equation:

$$\mathrm{DCIR} = R_{\mathrm{d}} + R_{\mathrm{i}} = \frac{V_1 - V_2}{I_1 - I_2}. \tag{2}$$

The advantage of this method is the capability of continuous online measurement during the charging process, thus obtaining real-time DCIR. There is no effect on the charging function since the current is always present and the battery has not been relaxed and shelved. DCIR is measured once every fixed time interval by this method during the charging process. It is possible to efficiently grasp the variation trend of DCIR while completing the charging.

B. Online Measurement Experiment

The battery test system (BTS) is adopted to experiment on the INR18650-30Q Li-ion battery produced by Samsung, and the configuration of the experimental prototype is shown in Fig. 3. The nominal specifications of INR18650-30Q are shown in Table I. The designed BTS employs the DSP TMS320F28055 as the main controller. The Arduino UNO module, which is based on the Atmel 8-bit MCU ATmega328, is adopted to store the experimental data on an SD card. The operating principle and configuration of BTS are described in detail in [26] and will not be repeated in this article.

TABLE I
NOMINAL SPECIFICATIONS OF INR18650-30Q

Item	Specification
Minimum discharge capacity	2950 mAh Charge: 1.50 A, 4.20 V, CCCV 150 mA cutoff Discharge: 0.2 C, 2.5 V discharge cutoff
Nominal voltage	3.6 V
Standard charge	CCCV, 1.50 A, 4.20 ± 0.05 V, 150 mA cutoff
Rated charge	CCCV, 4 A, 4.20 ± 0.05 V, 100 mA cutoff
Charging time	Standard charge : 180 min/150 mA cutoff Rated charge: 70 min/100 mA cutoff

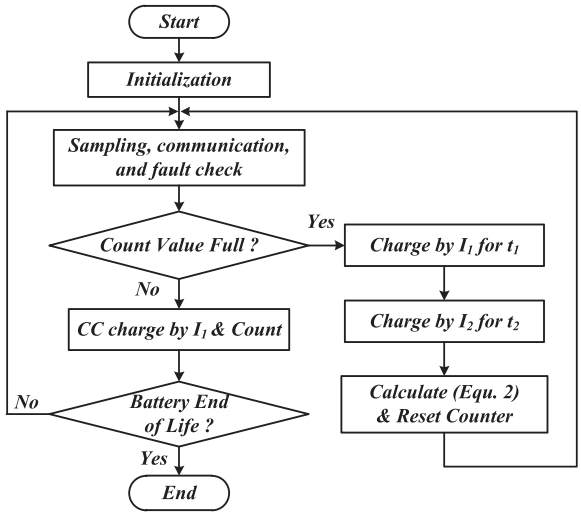

Fig. 4. Program flowchart of the battery online measurement.

Fig. 5. Battery is charged until it explodes.

Fig. 4 illustrates the program flowchart of the battery online measurement. The battery is CC charged with I_1, and a counter is adopted to ensure that the DCIR is measured at every fixed time interval. The current is resumed to I_1 for CC charging after the measurement is completed, and thus the cycle. The battery is charged with a 1 C current until it explodes ($I_1 = 1$ C), as shown in Fig. 5. During this process, the DCIR is measured every one-minute interval by the method shown in Fig. 2. The profiles of i_{bat}, V_{bat}, and corresponding V_{oc} are shown in Fig. 6(a). V_{oc} is simply estimated using V_1, I_1, and DCIR at each measurement. The DCIR online measurement results and fitted curve of five groups of batteries under identical experimental conditions are shown in Fig. 6(b). The battery can be divided into five operating stages according to the variation of V_{oc}. Strictly speaking, a

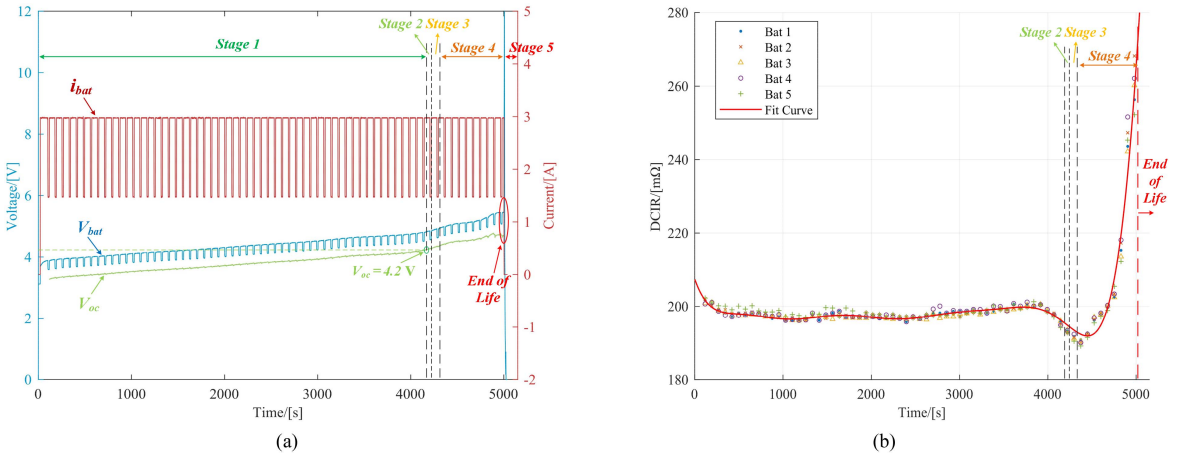

Fig. 6. Online measurement results of the charging process. (a) Current profile and corresponding voltage. (b) DCIR variation trend and its fitted curve.

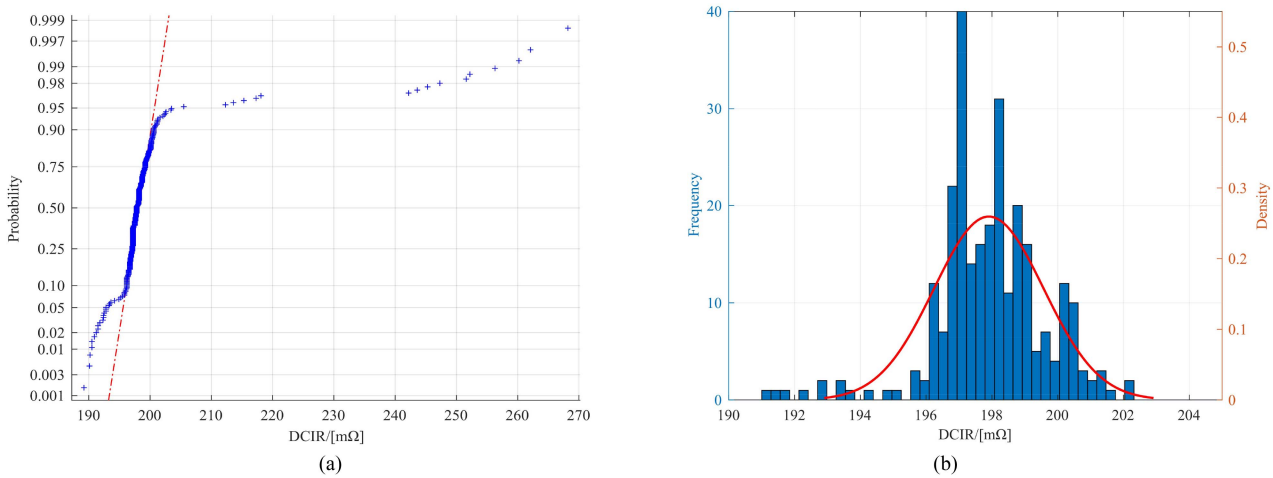

Fig. 7. (a) Q–Q plot of DCIR measurement data. (b) DCIR histogram and the fitted PDF of the Gaussian distribution.

Li-ion battery is overcharged when it is charged beyond Stage 1, i.e., 4.20 V. However, there are degrees of overcharging.

Stage 1 ($2.5 < V_{oc} < 4.2$)*:* The normal charging stage.

Stage 2 ($4.2 < V_{oc} < 4.25$)*:* Mild overvoltage. It is generally considered that a stage below 4.25 V can be not regarded as overcharging, which is acceptable. It is because the charging limit voltage of the Li-ion battery is 4.20 V $\pm$ 0.05 V.

Stage 3 ($4.25 < V_{oc} < 4.35$)*:* Moderate overvoltage. There is barely any change in the capacity of the battery after a moderate overcharge occurs, and its discharge capacity may be higher than a normal battery. However, it will shorten the cycle life of the battery in the long term, so this situation should be avoided as much as possible.

Stage 4 ($4.35 < V_{oc} < 4.68$)*:* Severe overvoltage. The impact of severe overcharge on the capacity and life of the battery is more serious than moderate overvoltage.

Stage 5 ($V_{oc} > 4.68$)*:* End of life. The chemical side reactions of overvoltage will lead to battery damage or safety problems. At this point, the battery is no longer usable, and in severe cases, it may even explode.

Fig. 7(a) shows the quantile–quantile plot (Q–Q plot) of the DCIR measurement data, where the marker "+" plots all the data points. The Q–Q plot is a probability plotting method that compares two probability distributions by plotting their quartiles against each other. The dashed line represents the reference line of the theoretical distribution, and if all sample points are around this reference line, it is rational to assume that the sample data obey a Gaussian distribution. Otherwise, a distribution other than Gaussian would introduce curvature in the Q–Q plot. As shown in Fig. 7(a), the data points in the middle part are basically distributed near the reference line, and only the data on both sides deviate significantly from the reference line. It means that the data in the middle part can be considered to obey a Gaussian distribution. It is verified in Fig. 6(b) that from the end of Stage 1 to Stage 5, the DCIR shows a trend of first decreasing and then increasing sharply, which corresponds to the deviation from the reference line in Fig. 7(a). The decrease in DCIR leads to a deviation of the data to the left from the reference line, and the increase in DCIR leads to a deviation of the data to the right from the reference line. In other words, it is rational to assume that the DCIR of Stage 1 obeys a Gaussian distribution. Then, the DCIR histogram of Stage 1 and the fitted probability density

function (PDF) of the Gaussian distribution can be plotted as shown in Fig. 7(b). Therefore, we can conclude that the DCIR measurement data of Li-ion batteries in the normal charging stage obey a Gaussian distribution.

III. Adaptive Fast Charging Strategy

A. Adaptive Control of Transition Point

At a constant battery capacity, the charging power marks the charging speed. It is possible to maintain the high-power charging state longer to improve the charging speed without raising the charging voltage and current. While the charging power in the CC mode is generally great than that in the CV mode, so the CC mode is the primary action period of fast charging. It is simple and effective to improve the charging speed by maximizing the CC mode operation time. Theoretically, it is possible to rearward shift the transition point of CC to CV by raising the reference voltage of the CV mode, thus lengthening the operation time of the CC mode. In practice, however, it is difficult to determine this transition point, an optimal and generally applicable point, by simply increasing the CV reference voltage. Combined with the conclusion in Section II, there is no need to find a specific expression for the relationship between DCIR and SOC, but rather to only focus on the variation of DCIR, which would reflect the current operating stage and status information of the battery. The idea is to employ CC to charge the battery, combined with DCIR online measurement at the same time. Then the DCIR-measured data in Stage 1 should obey a Gaussian distribution. Once the DCIR measurement data no longer obeys the Gaussian, which means the data deviates from the average value significantly, it can be considered that the battery is close to full charge or abnormal. At this time, the charging mode is immediately switched from CC to CV, thereby ensuring the safe operation of the battery.

The foundation for making a judgment by this method is to acquire the expectation and variance of the Gaussian distribution to which the data are subject. However, in the process of measurement, we can only estimate the uncertain parameters of the Gaussian with the sample information obtained from measurement. Assuming that all DCIR data obey a Gaussian distribution whose expectation is μ and variance is σ^2, which can be expressed as

$$\text{DCIR} \sim N\left(\mu, \sigma^2\right). \tag{3}$$

The DCIR is measured n times repeatedly and independently under the same experimental conditions, and the results are given as

$$r \triangleq [r_1, r_2, \ldots, r_{\mathrm{n}}]^{\mathrm{T}} \in \mathbb{R}^{\mathrm{n}}. \tag{4}$$

Then, the PDF of DCIR is represented as

$$f(r) = \frac{1}{\sqrt{2\pi}\sigma} e^{-\frac{(r-\mu)^2}{2\sigma^2}}. \tag{5}$$

The average value of the online measurements is expressed as

$$\bar{r} = \frac{1}{n}\sum_{i=1}^{n} r_i. \tag{6}$$

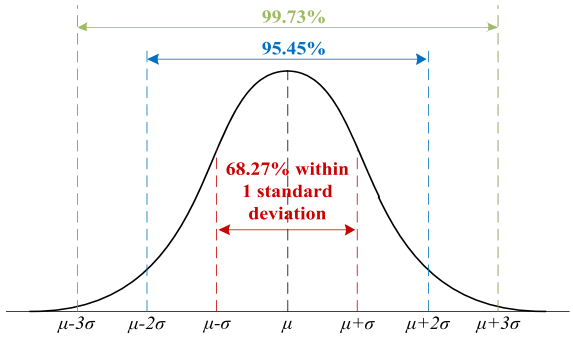

Fig. 8. Proportion of data deviation from the expectation for Gaussian distribution.

In the case that the distribution of DCIR is known, the uncertain parameters μ and σ^2 could be inferred according to the measured data adopting the maximum-likelihood estimation method, where the likelihood function of DCIR is

$$L(\mu, \sigma) = \prod_{i=1}^{n} f(r_i; \mu, \sigma) = \prod_{i=1}^{n} \frac{1}{\sqrt{2\pi}\sigma} e^{-\frac{(r_i-\mu)^2}{2\sigma^2}}. \tag{7}$$

The log-likelihood equation is represented as

$$\begin{cases} \frac{\partial}{\partial \mu} \ln L(\mu, \sigma) = \frac{1}{\sigma^2}\left[\sum_{i=1}^{n} r_i - n\mu\right] \\ \frac{\partial}{\partial \sigma^2} \ln L(\mu, \sigma) = -\frac{n}{2\sigma^2} + \frac{1}{2(\sigma^2)^2}\sum_{i=1}^{n}(r_i - \mu)^2 \end{cases}. \tag{8}$$

By making (8) equal to 0, the maximum-likelihood estimates of μ and σ^2 could be solved

$$\begin{cases} \hat{\mu} = \frac{1}{n}\sum_{i=1}^{n} r_i = \bar{r} \\ \hat{\sigma}^2 = \frac{1}{n}\sum_{i=1}^{n}(r_i - \bar{r})^2 \end{cases}. \tag{9}$$

Therefore, the measurements obey a Gaussian distribution with expectation $\hat{\mu}$ and variance $\hat{\sigma}^2$, which can be expressed as

$$r \sim N\left(\hat{\mu}, \hat{\sigma}^2\right). \tag{10}$$

Once the parameters of the Gaussian distribution are obtained, they can be used to determine whether the measured values are within the normal range. For the measured value r_{i}

$$P(\hat{\mu} - 3\hat{\sigma} \le r_i \le \hat{\mu} + 3\hat{\sigma}) \approx 0.9973. \tag{11}$$

It means that about 99.7% of the measured values should be located within a range less than $3\hat{\sigma}$ from $\hat{\mu}$ if they obey a Gaussian distribution, as shown in Fig. 8. Therefore, it is considered that when $r_{\mathrm{i}} > \hat{\mu} + 3\hat{\sigma}$ or $r_{\mathrm{i}} < \hat{\mu} - 3\hat{\sigma}$, the measured value significantly deviates from the expectation and no longer obeys $N(\hat{\mu},\hat{\sigma}^2)$, which indicates that the battery may be close to the full charge or overcharged. Then, the CC mode should be ended immediately and switched to CV at this point, which is the transition point of adaptive control.

B. Minimum Number of Measurements

The selection of the number of online measurements n for DCIR is another issue to be considered. To further improve the charging speed, n requires to be reduced as much as possible. The reason is that the online measurement contains two-level CC pulses, and if n is larger, it will result in a longer charging

time for small currents from the total charging time scale, which leads to a slower speed. However, if n is taken too small, it will cause inaccurate parameter estimates of the Gaussian distribution, which results in the incorrect determination of the transition point. In addition, it is actually not necessary to continuously measure DCIR during the entire Stage 1, since the same Gaussian could be represented by employing only a few data in that stage. Therefore, a more reasonable approach is to perform online measurements only in the last part of Stage 1. While satisfying the premise of high accuracy for the parameter estimates, the problem of determining $n_{\min}$ is formulated as the following constrained optimization problem:

$$\begin{aligned} &\text{minimize} \quad n \\ &\text{s.t.} \qquad \hat{\mu} = \mu \quad . \end{aligned} \tag{12}$$

Since the relationship between the estimated values and the actual Gaussian distribution expectations is ambiguous, the constraint is considered to transform into hypothesis testing. U-test, which is applicable to small sample data, is adopted to evaluate whether the sample data obtained from n tests are from the same Gaussian distribution as the overall data. The null hypothesis H_0 and the alternative hypothesis H_1 are proposed, and H_0 indicates that the measured data obey the same Gaussian distribution as the overall data.

$$H_0 : \hat{\mu} = \mu \quad H_1 : \hat{\mu} \neq \mu \ . \tag{13}$$

If H_0 is true, then $|\hat{\mu} - \mu|$ is smaller. It is not advisable to simply assume that H_0 is not true even if there is some discrepancy, because this may also be due to random factors. If $|\hat{\mu} - \mu|$ is large, H_0 is supposed to be rejected while accepting H_1. When H_0 is true

$$U = \frac{\hat{\mu} - \mu}{\hat{\sigma}/\sqrt{n}} \sim N(0, 1). \tag{14}$$

A small probability event A supporting H_1 holds is constructed, and it can be represented as

$$P(A) = P\left\{\frac{|\hat{\mu} - \mu|}{\hat{\sigma}/\sqrt{n}} \geq u_{\alpha/2}\right\} = \alpha \tag{15}$$

where α refers to the significance level and $u_{\alpha/2}$ is the corresponding bilateral critical value. Thus, the rejection region of H_0 is

$$|U| \geq u_{\alpha/2}. \tag{16}$$

Since A, as a small probability event, barely happens in a single test. If it does happen, we are justified in doubting the correctness of H_0 and consequently accepting H_1, which means that the distribution of DCIR cannot be expressed by this estimation value. Therefore, n ought to be increased to perform the hypothesis testing again until H_0 is accepted, at which point n is equal to $n_{\min}$. The flowchart of the algorithm for determining $n_{\min}$ is shown in Fig. 9.

The confidence level 1-α was adopted to ensure that the confidence interval contains the true value. 1-α reflects the reliability of the interval estimation, while the length of the confidence interval indicates the accuracy of the estimation. The fitted expectation of multiple groups of DCIR in Fig. 6 is calculated as μ, and $\alpha = 0.05$ is taken. When $n \geq 6$, $|U| < u_{\alpha/2} = 1.96$, so H_0 is accepted, and therefore $n_{\min}$ is equal to 6.

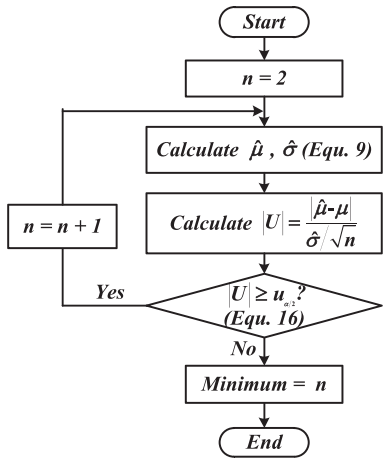

Fig. 9. Flowchart of the algorithm for determining the minimum number of measurements.

C. Specific Implementation of the Charging Strategy

According to the above experiments and analysis, in the case of 1C charging current, the previous DCIR measurement where the battery reaches full charge state is taken as the starting point, and count forward six points, at which V_{oc} is exactly slightly more than 4.1 V. For the purpose of ensuring at least six measurements of DCIR before the battery reaches full charge and preventing the battery from overcharging above Stage 2, it is necessary to assure that measurements are started at least before this point. Then, it is feasible to enter the online measurement stage (OMS) with DCIR measurements once per minute when $V_{\text{oc}} = 4.1$ V. $\hat{\mu}$ and $\hat{\sigma}^2$ are calculated after obtaining 6 measurements, and they are taken as the criterion for adaptive control of the transition point. After that, the DCIR measurement continues until $r_{\text{i}} > \hat{\mu} + 3\hat{\sigma}$ or $r_{\text{i}}\ \hat{\mu} - 3\hat{\sigma}$ when it switches to CV mode immediately.

Moreover, the proposed method is equally applicable for the case below 1C, since its OMS lasts longer. However, it is necessary to measure DCIR once before the OMS, after which the value is employed to estimate V_{oc}. A simple approach is to carry out the measurement when V_{bat} reaches 4.2 V, which point is the transition point in the traditional CC-CV charging method. When V_{bat} first reaches 4.2 V, the DCIR is calculated according to (2) by applying the online measurement method shown in Fig. 2. From the conclusions drawn in Section II, it is clear that the DCIR measurements during the normal charging stage obey a Gaussian distribution. The variation of DCIR is slight until the battery is fully charged. Therefore, the DCIR measured at $V_{\text{bat}} = 4.2$ V can be employed to estimate the V_{oc} during the charging process afterward, as shown in (17). The schematic diagram of the proposed fast charging strategy based on transition point adaptive control and $n_{\min}$ is shown in Fig. 10.

$$V_{\text{oc}} = V_1 - I_1 \cdot \text{DCIR}. \tag{17}$$

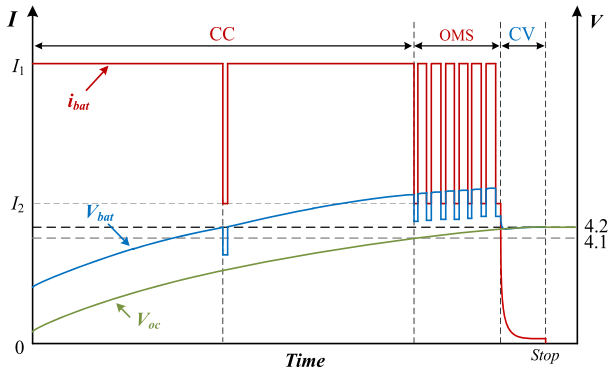

Fig. 10. Schematic diagram of the proposed fast charging strategy for Li-ion batteries.

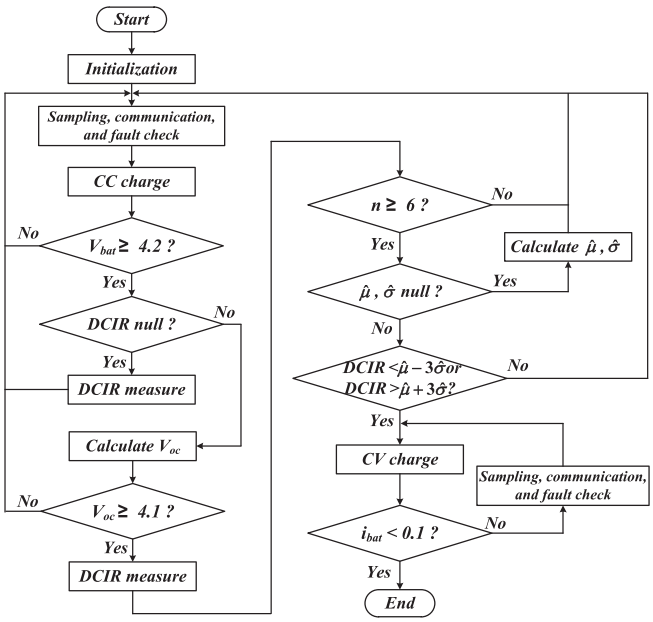

Fig. 11. Program flowchart of the proposed fast charging strategy.

The proposed fast charging strategy firstly adopts CC mode for charging, then enters OMS when V_{OC} reaches 4.1 V, and finally switches to 4.2-V CV mode once the DCIR deviates from the Gaussian distribution. Compared with the conventional CC-CV method, the proposed strategy maximizes the charging time of CC mode and incorporates an OMS for real-time monitoring of DCIR, which improves the charging speed and prevents the battery from overcharging. Actually, the OMS is implemented by two-level pulses and the duration of the low-level pulses is short. Hence, the charging speed in this stage differs little from the CC mode, which is also regarded as the CC stage in a broad sense. The program flowchart of the proposed fast charging strategy is shown in Fig. 11.

It is not required to measure the DCIR with great accuracy for the proposed method, and the prerequisites to be identified are the rated capacity of the battery and the charging cutoff voltage. The focus of the proposed strategy is on the trend of DCIR rather than on the actual value. When the DCIR measurement changes dramatically and no longer obeys a Gaussian distribution, it indicates that the battery state has also changed accordingly. In other words, we are concerned with the degree that the DCIR

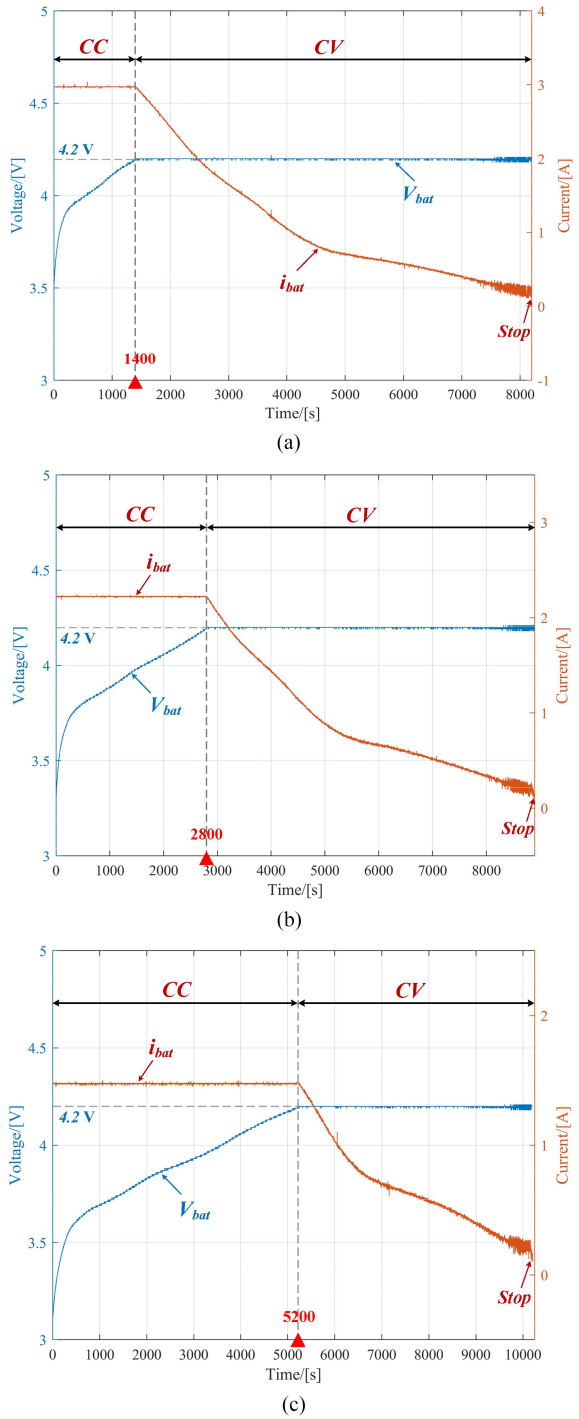

Fig. 12. Current profiles and corresponding voltages based on the traditional CC-CV charging strategy for (a) 1C, (b) 0.75C, and (c) 0.5C.

measurements deviate from the expectation under the same criteria (same parameters and model). As long as it is ensured that the DCIR is measured based on the same standard, then the error of all measurements relative to the exact value is also uniform, and the trend of DCIR changes can correctly reflect the change in battery state. Based on this, it is possible to employ statistical methods to determine the transition point of fast charging. Therefore, the proposed strategy is not sensitive to the accuracy of the DCIR measurements. In the case of measuring DCIR once

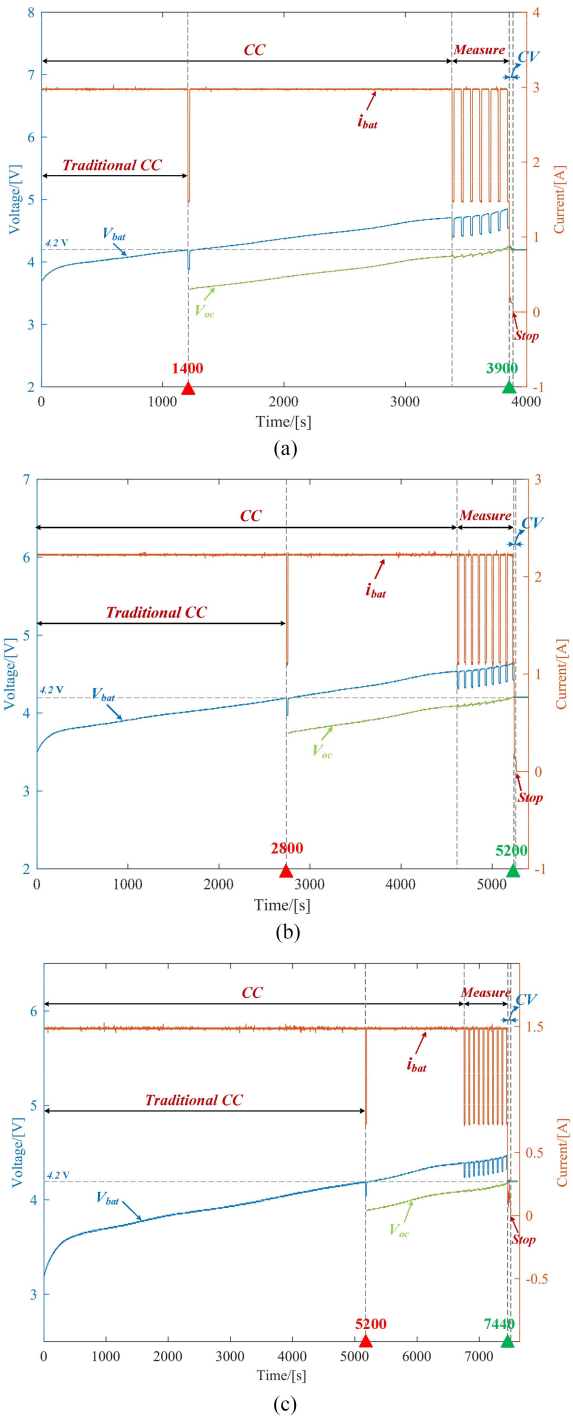

Fig. 13. Current profiles and corresponding voltages based on the proposed fast charging strategy for (a) 1C, (b) 0.75C, and (c) 0.5C.

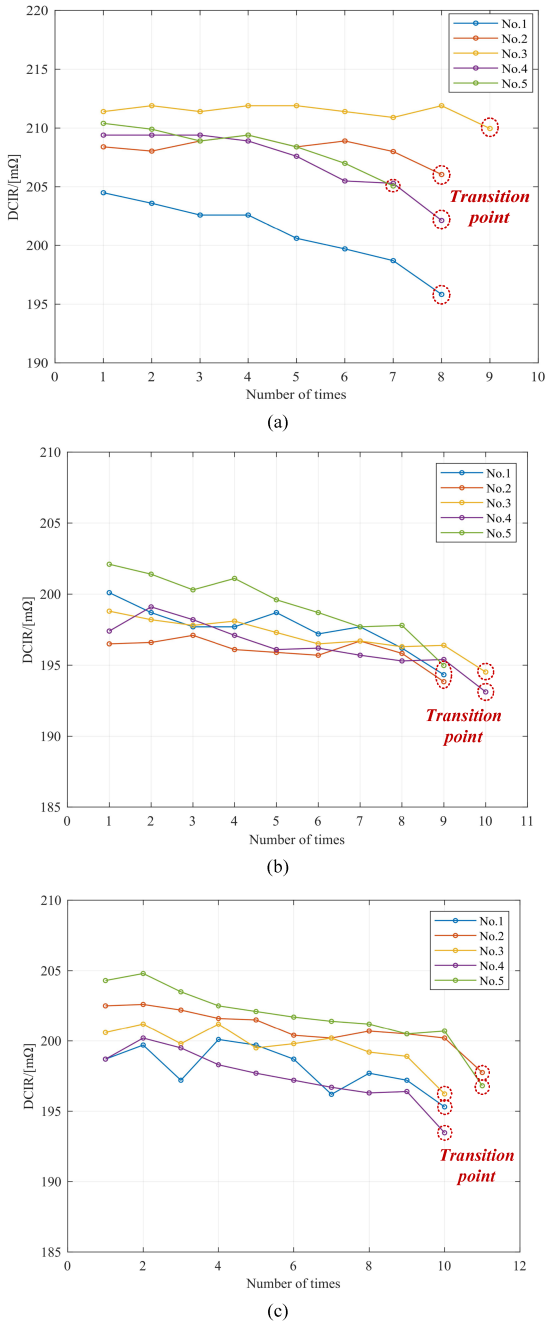

Fig. 14. DCIR variations in OMS and the corresponding transition points (a) 1C, (b) 0.75C, and (c) 0.5C.

per minute, t_2 can be taken as small as possible to minimize the influence of the measurement process on the charging speed. However, at the same time, to avoid excessive errors, the battery terminal voltage should not change significantly anymore after t_2, which is obtained based on engineering experience after several experimental observations. In the case that the proposed method does not require high accuracy, the simplest tradeoff is to take $I_1 = 2I_2$ and $t_1 = t_2 = 15$ s.

IV. Experimental Verification

Based on the BTS shown in Fig. 3, the INR18650-30Q Li-ion battery is charged by the traditional CC-CV method at 1C, 0.75C, and 0.5C, whereas the current profiles and corresponding voltages are shown in Fig. 12(a)–(c), respectively. It is observed that the traditional CC-CV method consumes about 136.4 min, 148.2 min, and 180 min to fully charge the battery at 1C, 0.75C, and 0.5C, respectively. The red triangle on the time axis in Fig. 12 indicates the transition point of the traditional method, and the duration of the CC mode accounts for approximately 17.09%, 31.4%, and 48.2% of the total charging time, respectively.

TABLE II
EXPERIMENTAL DATA BASED ON THE PROPOSED FAST CHARGING STRATEGY

C-rate	No.	$\hat{\mu}$	$\hat{\sigma}$	Permissive extent	Transition point (mΩ)	Charging time (mins)	The voltage after 30 min
1C	1	202.31	1.66	(197.33, 207.29)	195.83	65	4.21
	2	208.66	0.46	(207.27, 210.04)	206.05	64.5	4.18
	3	211.67	0.25	(210.93, 212.40)	209.96	66.8	4.17
	4	208.32	1.50	(203.80, 212.86)	202.14	65.5	4.19
	5	209.02	1.11	(205.74, 212.38)	205.07	64.2	4.20
0.75C	1	198.40	0.96	(195.51, 201.29)	194.33	87.5	4.20
	2	196.12	0.46	(194.74, 197.50)	193.84	85.7	4.19
	3	197.79	0.75	(195.54, 200.04)	194.52	87.2	4.21
	4	197.32	1.03	(194.23, 200.41)	193.12	86.5	4.20
	5	200.31	1.11	(196.98, 203.64)	194.98	86.1	4.17
0.5C	1	199.04	0.96	(196.16, 201.94)	195.31	125.7	4.19
	2	201.80	0.78	(199.48, 204.16)	197.75	128.4	4.2
	3	200.37	0.69	(198.30, 202.44)	196.23	125.3	4.19
	4	198.65	1.02	(195.59, 201.71)	193.47	127.6	4.21
	5	203.13	1.15	(199.68, 206.58)	196.81	125.5	4.18

TABLE III
PERFORMANCE COMPARISON OF THE PROPOSED STRATEGY WITH OTHER STRATEGIES

Strategy	Maximum C-rate	Battery capacity (mAh)	Charging time (min)	Final SOC (%)	Time saved (%)
CC-CV	1C	3000	136.4	100	N/A
	0.75C		148.2		
	0.5C		180		
Proposed	1C	3000	65.2	100	52.20
	0.75C		86.6		41.57
	0.5C		126.5		29.72
Constant-Temperature CV [3]	2C	2500	69.5	100	18.24
Improved CC-CV [7]	1C	2000	60	100	41.20
MSCC-5 [10]	1C	2400	87.06	100	12.0
MSCC-5 [13]	1.44C	2200	51	88	56.70
Pulse [17]	0.5C	600	70.7	100	47.6
Constant Average Current [27]	0.667C	750	150	100	17.10
MSCC-4 [28]	1.8C	5000	60	94.8	21.03

To verify the validity of the proposed fast charging strategy, the same Li-ion battery is charged at 1C, 0.75C, and 0.5C, whereas the current profiles and corresponding voltages are shown in Fig. 13(a)–(c), respectively. It can be seen that the proposed strategy consumes about 65.2 min, 86.6 min, and 126.5 min to fully charge the battery, respectively. The green triangle on the time axis in Fig. 13 signifies the transition point of the proposed method. Compared with the traditional CC-CV, the transition point of the proposed strategy is shifted to the right. The duration of the CC mode is close to 100% of the total charging time at 1C, 0.75C, and 0.5C. Fig. 13 indicates that the proposed fast charging strategy maximizes the operating time of the CC mode by adaptive control of the transition point based on the DCIR variation, which leads to a significant improvement in the charging speed of the Li-ion batteries. Moreover, the proposed strategy is effective for charging currents of 1C and below, as well as the higher is C-rate, the faster the charging speed. Fig. 14 shows the DCIR variations in the OMS and the corresponding transition points at 1C, 0.75C, and 0.5C, respectively. The transition point varies depending on the C-rate and the battery state, resulting in a discrepancy in the number of measurements, which demonstrates the feasibility and flexibility of the transition point adaptive control.

The 15 groups of experimental data for charging the battery from 2.5 V to full state by the proposed strategy are shown in Table II, where the permissive extent represents the interval of $\hat{\mu} - 3\hat{\sigma} \leq r_i \leq \hat{\mu} + 3\hat{\sigma}$. When the DCIR is outside this interval, it indicates a significant deviation from the expectation and ought to switch from CC to CV immediately. Throughout the charging process by the proposed method, it is approximately equivalent to charging the Li-ion battery to the rated capacity with CC mode since the operating time of CV mode is negligible. It is confirmed by the data in Table II. V_{bat} are measured again after shelving for 30 min, and it is found that all batteries are fully charged and without overcharging, which demonstrates the high accuracy and reliability of the proposed strategy.

Table III shows the performance comparison of the proposed fast charging strategy with other charging strategies. Compared to the conventional CC-CV, the proposed strategy saves 52.2%, 41.57%, and 29.72% of the total charging time at 1C, 0.75C, and 0.5C, respectively, with higher time savings at higher C-rates. The charging speed of the proposed strategy is further improved

compared to previous works. The time-saving rate of [7] with 1C current is 41.2%. In contrast, the time-saving rate for the proposed strategy with 1C is 52.2%. In addition, although the time-saving rate of [13] is slightly better than the 52.2% for the proposed method, its charging target SOC is 88%, which has a limited application range. The battery capacity of [17] is too low and is not applicable in the case of other C-rates due to temperature rise. Therefore, in summary, the proposed strategy in this article is superior by taking into account speed and safety, which effectively improves the charging speed while preventing overcharging.

V. Conclusion

In this article, an adaptive fast charging strategy for Li-ion batteries considering the variation of DCIR is proposed, which applies to mobile applications. The online measurement experiment reveals that the DCIR, as a key parameter for measuring the performance of Li-ion batteries, obeys Gaussian distribution during the normal charging stage. However, the DCIR no longer obeys Gaussian distribution once the battery is fully charged. The expectation and variance of the Gaussian distribution obeyed by DCIR are obtained by the maximum-likelihood estimation method, and the estimates are employed for adaptive control of the optimal transition point. When the DCIR deviates significantly from the expectation, the battery is considered close to full charge and immediately switches from CC to CV mode. Under the premise of satisfying the high accuracy for the parameter estimates, a constrained optimization problem is established to determine the DCIR minimum number of measurements. To simplify the problem, the constraints are transformed into hypothesis testing to evaluate the Gaussian distribution of the data samples. The CC operating time is maximized based on $n_{\min}$ and the adaptive control of the transition point, and the specific implementation of the fast charging strategy is presented. The experiments verify the validity of the proposed method. The results show that compared with the CC-CV method, the proposed strategy saves 52.2%, 41.57%, and 29.72% of the charging time at 1C, 0.75C, and 0.5C, respectively, which effectively improves the charging speed and prevents overcharging. Compared with the previous works, the proposed strategy is superior by taking into account speed and safety.

References

[1] P. Liu and C. Yen, "A fast-charging switching-based charger with adaptive hybrid duty cycle control for multiple batteries," *IEEE Trans. Power Electron.*, vol. 32, no. 3, pp. 1975–1983, Mar. 2017.

[2] Q. Ouyang, G. Xu, H. Fang, and Z. Wang, "Fast charging control for battery packs with combined optimization of charger and equalizers," *IEEE Trans. Ind. Electron.*, vol. 68, no. 11, pp. 11076–11086, Nov. 2021.

[3] L. Patnaik, A. V. J. S. Praneeth, and S. S. Williamson, "A closed-loop constant-temperature constant-voltage charging technique to reduce charge time of lithium-ion batteries," *IEEE Trans. Ind. Electron.*, vol. 66, no. 2, pp. 1059–1067, Feb. 2019.

[4] H. Tu, H. Feng, S. Srdic, and S. Lukic, "Extreme fast charging of electric vehicles: A technology overview," *IEEE Trans. Transp. Electrific.*, vol. 5, no. 4, pp. 861–878, Dec. 2019.

[5] H. Li, X. Zhang, J. Peng, J. He, Z. Huang, and J. Wang, "Cooperative CC–CV charging of supercapacitors using multicharger systems," *IEEE Trans. Ind. Electron.*, vol. 67, no. 12, pp. 10497–10508, Dec. 2020.

[6] Z. Li, H. Liu, Y. Tian, and Y. Liu, "Constant current/voltage charging for primary-side controlled wireless charging system without using dual-side communication," *IEEE Trans. Power Electron.*, vol. 36, no. 12, pp. 13562–13577, Dec. 2021.

[7] Y. Jung et al., "A fast and highly accurate battery charger with accurate built-in resistance detection," *IEEE Trans. Power Electron.*, vol. 33, no. 12, pp. 10051–10054, Dec. 2018.

[8] D. Anseán et al., "Fast charging technique for high power lithium iron phosphate batteries: A cycle life analysis," *J. Power Sources*, vol. 239, pp. 9–15, 2013.

[9] D. Anseán et al., "Fast charging technique for high power LiFePO4 batteries: A mechanistic analysis of aging," *J. Power Sources*, vol. 321, pp. 201–209, 2016.

[10] A. B. Khan and W. Choi, "Optimal charge pattern for the high-performance multistage constant current charge method for the Li-ion batteries," *IEEE Trans. Energy Convers.*, vol. 33, no. 3, pp. 1132–1140, Sep. 2018.

[11] L. Jiang et al., "Optimization of multi-stage constant current charging pattern based on Taguchi method for Li-ion battery," *Appl. Energy*, vol. 259, Feb. 2020, Art. no. 114148.

[12] C.-H. Lee, C.-Y. Hsu, S.-H. Hsu, and J.-A. Jiang, "Effect of weighting strategies on Taguchi-based optimization of the four-stage constant current charge pattern," *IEEE Trans. Aerosp. Electron. Syst.*, vol. 57, no. 5, pp. 2704–2714, Oct. 2021.

[13] S. Wang and Y. Liu, "A PSO-based fuzzy-controlled searching for the optimal charge pattern of Li-ion batteries," *IEEE Trans. Ind. Electron.*, vol. 62, no. 5, pp. 2983–2993, May 2015.

[14] H. Min et al., "Research on the optimal charging strategy for Li-ion batteries based on multi-objective optimization," *Energies*, vol. 10, no. 5, pp. 709, May 2017,.

[15] Y. Li et al., "Optimized charging of lithium-ion battery for electric vehicles: Adaptive multistage constant current–constant voltage charging strategy," *Renewable Energy*, vol. 146, pp. 2688–2699, 2020.

[16] B. Kwak, M. Kim, and J. Kim, "Add-on type pulse charger for quick charging Li-ion batteries," *Electronics*, vol. 9, no. 2, Jan. 2020, Art. no. 227.

[17] J. M. Amanor-Boadu, A. Guiseppi-Elie, and E. Sánchez-Sinencio, "Search for optimal pulse charging parameters for Li-ion polymer batteries using Taguchi orthogonal arrays," *IEEE Trans. Ind. Electron.*, vol. 65, no. 11, pp. 8982–8992, Nov. 2018.

[18] D. Kannan and M. Weatherspoon, "The effect of pulse charging on commercial lithium nickel cobalt oxide (NMC) cathode lithium-ion batteries," *J. Power Sources*, vol. 479, Dec. 2020, Art. no. 229085.

[19] C. Zou, X. Hu, Z. Wei, T. Wik, and B. Egardt, "Electrochemical estimation and control for lithium-ion battery health-aware fast charging," *IEEE Trans. Ind. Electron.*, vol. 65, no. 8, pp. 6635–6645, Aug. 2018.

[20] C. Zou, X. Hu, Z. Wei, and X. Tang, "Electrothermal dynamics-conscious lithium-ion battery cell-level charging management via state-monitored predictive control," *Energy*, vol. 141, pp. 250–259, 2017.

[21] J. Liu, G. Li, and H. K. Fathy, "An extended differential flatness approach for the health-conscious nonlinear model predictive control of lithium-ion batteries," *IEEE Trans. Control Syst. Technol.*, vol. 25, no. 5, pp. 1882–1889, Sep. 2017.

[22] B. G. Carkhuff, P. A. Demirev, and R. Srinivasan, "Impedance-based battery management system for safety monitoring of lithium-ion batteries," *IEEE Trans. Ind. Electron.*, vol. 65, no. 8, pp. 6497–6504, Aug. 2018.

[23] J. Ahn and B. K. Lee, "High-efficiency adaptive-current charging strategy for electric vehicles considering variation of internal resistance of lithium-ion battery," *IEEE Trans. Power Electron.*, vol. 34, no. 4, pp. 3041–3052, Apr. 2019.

[24] K. S. Song, S.-J. Park, and F.-S. Kang, "Internal parameter estimation of lithium-Ion battery using AC ripple with DC offset wave in low and high frequencies," *IEEE Access*, vol. 9, pp. 76083–76096, 2021.

[25] D. Stroe, M. Swierczynski, S. K. Kær, and R. Teodorescu, "Degradation behavior of lithium-ion batteries during calendar ageing—The case of the internal resistance increase," *IEEE Trans. Ind. Appl.*, vol. 54, no. 1, pp. 517–525, Jan./Feb. 2018.

[26] Y. Wang, S.-Y. Kim, Y. Chen, H. Zhang, and S.-J. Park, "An SMPS-based lithium-ion battery test system for internal resistance measurement," *IEEE Trans. Transp. Electrific.*, to be published, doi: 10.1109/TTE.2022.3178981.

[27] K. Chung, S.-K. Hong, and O.-K. Kwon, "A fast and compact charger for an Li-ion battery using successive built-in resistance detection," *IEEE Trans. Circuits Syst. II, Exp. Briefs*, vol. 64, no. 2, pp. 161–165, Feb. 2017.

[28] T. Vo, X. Chen, W. Shen, and A. Kapoor, " New charging strategy for lithium-ion batteries based on the integration of Taguchi method and state of charge estimation," *J. Power Sources*, vol. 273, pp. 413–422, 2015.

Yipei Wang (Graduate Student Member, IEEE) received the B.S. degree in smart grid information engineering and the M.S. degree in electrical engineering from Qingdao University of Science and Technology, Qingdao, China, in 2017 and 2020, respectively. He is currently working toward the Ph.D. degree in electrical engineering with Chonnam National University, Gwangju, South Korea.

His research interests include dc–dc converters and applications for battery charger converters.

Ancheng Liu received the B.S. degree in electrical engineering and automation from Hebei University of Engineering, Hebei, China, in 2018, and the M.S. degree in electrical engineering from Qingdao University of Science and Technology, Qingdao, China, in 2021. He is currently working toward the Ph.D. degree in electrical engineering with Chonnam National University, Gwangju, South Korea.

His research interests include dc–dc converters and vehicle-to-grid (V2G).

Yaochen Zhu received the B.S. degree in electrical engineering from the Korea National University of Transportation, Chungju-si, South Korea, in 2020. He is currently working toward the master's degree in electrical engineering with Chonnam National University, Gwangju, South Korea.

His current research interests include dc–dc converters and dynamic voltage restorer (DVR).

Hailong Zhang (Member, IEEE) received the B.S. degree in electronic engineering and automation from China Petroleum University, Dongying, China, in 2013, the M.S. degree in control theory and control engineering from Qingdao University of Science and Technology, Qingdao, China, in 2016, and the Ph.D. degree in electrical engineering from Chonnam National University, Gwangju, South Korea, in 2020.

He is currently a Lecturer with the Department of Information and Control Engineering, Qingdao University of Technology, Qingdao, China. His research interests include wireless power transfer systems for unmanned aerial vehicles (UAVs), power conversion systems for electric vehicles (EVs), and renewable energy storage systems.

Yafei Chen (Member, IEEE) received the B.S. degree in electronic information engineering from Southwest Jiaotong University, Chengdu, China, in 2012, the M.S. degree in control theory and control engineering from the Qingdao University of Science and Technology, Qingdao, China, in 2016, and the Ph.D. degree in electrical engineering from Chonnam National University, Gwangju, South Korea, in 2020.

He is currently a Lecturer with the Department of Electrical and Information Engineering, Zhengzhou University of Light Industry, Zhengzhou, China. His research interests include wireless power transfer for EVs and UAVs, topology, modeling and control of power converters, and applications for battery charger converters.

Sung-Jun Park (Member, IEEE) received the B.S., M.S., and Ph.D. degrees in electrical engineering and the Ph.D. degree in mechanical engineering from Pusan National University, Busan, South Korea, in 1991, 1993, 1996, and 2002, respectively.

From 1996 to 2000, he was an Assistant Professor with the Department of Electrical Engineering, Koje College, Koje, South Korea. From 2000 to 2003, he was an Assistant Professor with the Department of Electrical Engineering, Tong-Myong College, Busan, South Korea. Since 2003, he has been a Professor with the Department of Electrical Engineering, Chonnam National University, Gwangju, South Korea. His research interests include power electronics, motor control, mechatronics, and micromachine automation.